EB2019-IBC-010

ADAPTIVE WHEEL SLIDE PROTECTION ALGORITHMS

Frea, Matteo*; Tione, Roberto
Faiveley Transport Italy (Wabtec)

KEYWORDS – WSP, Wheel Slide Protection, Adaptive, Algorithm, Adhesion

INTRODUCTION

Railway transport is generally acknowledged for its low cost, environmental friendliness, energy efficiency, safety and fast speed, both for short and medium distances, compared to other means of transportation. The adhesion between train wheels and the rail has a key role on all these factors. As railway systems are open systems, the adhesion between the wheel and rail is inevitably affected by contaminants reducing the capability of the train to transfer force to the rail, thus reducing the efficiency of traction and braking processes.

Rolling Stock electronic control systems generally include slip control subsystems, available to control possible sliding in case of degraded adhesion when the vehicle is in the traction phase and when it is in the braking phase. These subsystems are known as Antiskid or Antislide, or even Wheel Slide Protection, hereinafter referred to as WSP.

SUMMARY

What is discussed here below is characteristic of a WSP system, a subject expert can easily translate the concepts expressed to an Antiskid system (traction control during slide), to which the present article is also extended.
After a state of the art of the current adhesion control strategies and their limits, an overview on the adaptive filters is presented. The application of such algorithm for a torque control architecture will be outlined with different solution. Then, the test environment will be introduced, and the adaptive algorithm will be tested in such environment following a rigorous procedure.

METHODOLOGY

An adhesion control system is described in Figure 1, the illustration refers to a slip control system per axle. The electronic control system typically based on microprocessor architectures, receives tachometric signals related to the instantaneous angular velocity of each axle *A1 ... An* by means of speed sensors *SS1 ... SSn*.

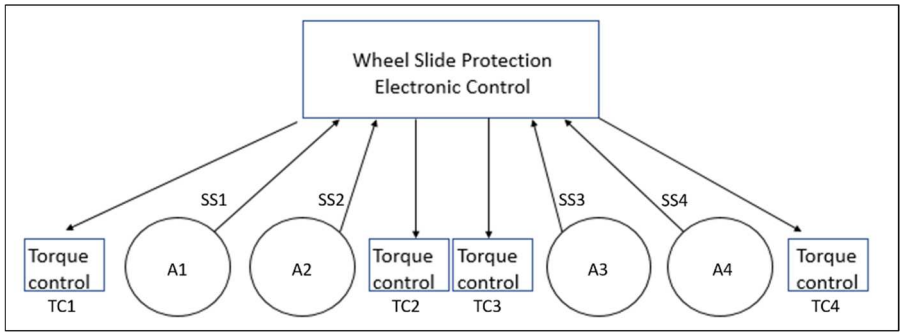

Figure 1: Axle based architecture schematic of an anti-skid/anti-slide control system.

By means of torque control means *TC1* ... *TCn*, the adhesion control system modulates the torque, individually for each axle, according to the appropriate algorithm if in case of application of torque, during traction or braking.
In a degraded adhesion situation, one or more axles may enter in a situation of possible sliding. The Slip control system reacts preventing the total blockage of the axles, and possibly bringing each axle into a controlled sliding situation until the best recovery of the available adherence, and in any case during the whole lasting of the degraded adhesion situation.

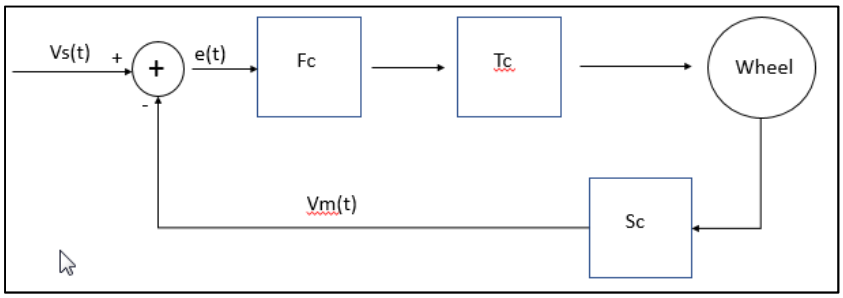

Figure 2: Anti-skid/anti-slide control's architecture for a single axle

Figure 2 shows a generic block diagram related to the control of a single axle: the error *e(t)* is calculated as the difference between the reference speed *Vs(t)* at which the adhesion control system aims to keep the sliding, and the speed of *Vm(t)* measured by the *SS* detection system and conditioned by the *SC* acquisition/conditioning system. The control algorithm *Fc* generates the torque request (or torque variation request) for the *Tc* torque control system in order to minimise the error *e(t)*.

It is well known that the *Fc* algorithm can be realized, for example, through State Diagrams algorithms rather than conventional PID control algorithms or Fuzzy Logic structures. The *Fc* algorithm has the objective of maintaining the axle which has started a sliding phase, at a so-called "sliding" speed equal to a fraction of the vehicle speed, said sliding speed also known as *set-point speed.*

Whilst these algorithms can fulfil their scope in a recognised satisfactory way, they require parameter calibration procedures in order to make said algorithms stable, avoiding system oscillations or, in the case of WSP systems, excessive oscillations of the instantaneous speed of the controlled axle around the so-called *set-point speed.* Said oscillations are known cause of braking distance elongation and huge air consumption from the pneumatic brake reservoirs.

As known to experts in the field of Wheel Slide Protection systems, the calibration of the parameters is a complex process requiring several days of experts work and trains immobilisation for the tests, and said complexity increases with the increase of the surrounding environmental variables fluctuations.

In the case of an adherence control system, one of the system variables having a wide range of variation is the friction force

$$Fa\ (t) = \mu\ (\delta,t) \cdot m \cdot g$$

acting at the point of contact between the wheel and the rail, as shown in Figure 3.

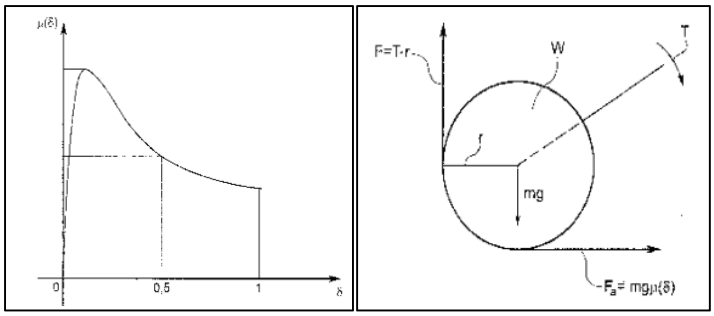

*Figure 3. Left: Adhesion curve representing the wheel-rail adhesion coefficient (y axis) in function of **δ** that is the wheel's relative slide (x axis). Right: Diagram of forces' vectors acting on the wheelset.*

Under normal vehicle weight conditions, pseudo-static $\mu(\delta)$ values $(\delta \approx 0)$ such to trigger sliding phenomena are close to $\mu\ (\approx 0) = 0.09$ and may go down to values around $\mu\ (\approx 0) = 0.01$ or even lower in case of rotten leaves or mix of water and rust. This variation corresponds to an equivalent gain change circa *20dB*. Moreover, in the case of some contaminants, the sliding action may cause sudden fast variations of the instantaneous value of $\mu(\delta)$ in the range $\mu\ (\approx 0) < \mu(\delta) < 0.5 * \mu\ (\approx 0)$, corresponding to circa 6dB. Furthermore, the *m* weight value on the axle can vary both statically between tare and full load and dynamically during the sliding due to the mass transfer effect, both at vehicle and at bogie level, with consequent redistribution of the weights between the four axles. During the simultaneous sliding of several axles, there is a phenomenon known as "rail cleaning", for which a sliding axle produces friction at the point of contact between the wheel and the rail, injecting energy, and consequently partially cleaning the rail, increasing the value $\mu(\delta)$ for the next axle. This phenomenon causes consecutive axles to meet at the same time different instantaneous adhesion values. Furthermore, as the speed decreases, the friction coefficient between disc and brake pad (in the case of disc brakes) or between the wheel and the log (in the case of a braking shoe), can undergo substantial variations. Lastly, a system that intends to manage torque controls articulated between several actuators as described in Figure 2, have to adapt to different transfer functions and time constants, in real time. The coexistence of such variations requires applying a "non-rigid" calibration that accepts the whole spectrum of variations, with the consequence of not having an accurate and reactive control to rapid environmental variations, or an adaptive calibration "mapped" through a "lookup table" of parameters selected in real time according to one or more of the environmental variables described above, as for example claimed in the patent [6].

The control algorithm described in this article is based on techniques achieving the calibration and dynamic correction of the parameters of the sliding control, performed in real time, and not previously mapped through pre-tuned parameters. For the described purpose, techniques known as Adaptive Filters are used. Various types of Adaptive Filters are suitable for the claimed application. The present article illustrates the specific application of a typology of Adaptive Filters known as LMS (Least Mean Square) Adaptive Filters.

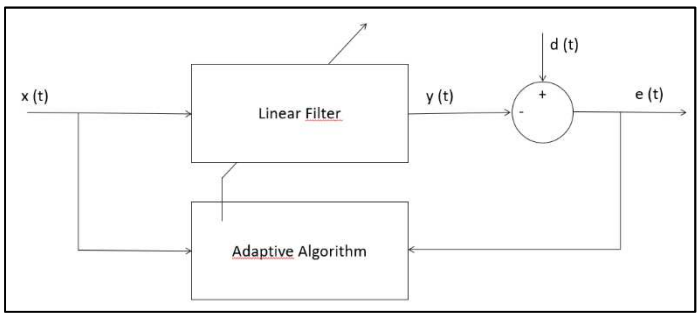

Figure 4: Least Mean Square adaptive filter structure.

Figure 5 illustrate a typical LMS Adaptive Filter structure; *x (t)* and *y (t)* represent the input and the output of the variable coefficients filter. The most known filter structure is the FIR (Finite Impulse Response) structure, nevertheless it is possible to utilize as well IIR (Infinite Impulse Response) structures. The error *e (t)* is calculated between the reference signal *d (t)* and the output *y (t)* and is used by the Adaptive Algorithm to calibrate the filter coefficients, to minimize the error between the output *y (t)* and the reference signal *d (t)*.

In the following description the definition of the time variable *t* previously used will be redefined with the letter *T* to indicate that the time is discrete, i.e. that the system operates for finite sampling with period *T*.

Referring to [1] and [2], an application of an adaptive filter to the adaptive control of the sliding of an axle belonging to a railway vehicle, claimed by the present article, is shown in Figure 5.

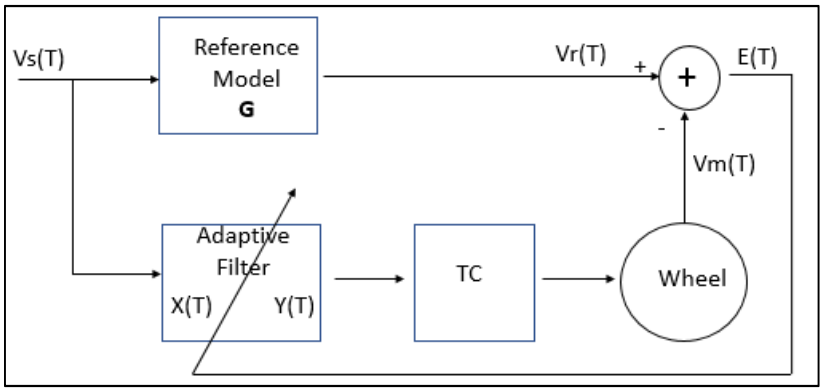

Figure 5: Least Mean Square adaptive filter applied on a slide control architecture.

The system set point is the reference speed *Vs(T)* at which the adhesion control system aims to keep the sliding. *Vs(T)* is sent both to a reference system model *G*, and to the Adaptive Filter. The Adaptive Filter output *Y(T)* is the Torque Request to be applied to the Torque Control in order to continuously minimize the error *E(T)*, calculated as difference between the output of the reference system model *G* and the real speed of the axle to be controlled. Ideally, the reference system model *G* should assume the "unit multiplier" form *G=1*, a more significant system close to reality can be a second order system approximating the expected model of the sequence *Tc, Wheel*. Finally, the error *E(T)* is used into the Adaptive Filter to perform the continuous correction of the coefficients, until *E(T)* is minimized.

The shown overall architecture aims to self-adapt at any combination of the previously described system variables change ($\mu(\delta)$, weight, friction pair adhesion coefficient), and to continuously recalibrate itself according to sudden variations of the adhesion coefficient $\mu(\delta)$ occurring during the sliding.

Because the system variables ($\mu(\delta)$, weight, friction pair adhesion coefficient) almost change at every brake application, it is expected the Adaptive Filter finds the best possible tuning in fractions of second, at every beginning of sliding events. Longer tuning times risk to allow over sliding events bringing to wheels flats.

It is a known art relative to the use of Adaptive Filters based on LMS structures, that a fast stabilization of the filter coefficients occurs in the presence of an input signal *X(T)* with a harmonic content equivalent or higher to the band of the process to be controlled. Unluckily, in the case of a setpoint represented by *Vs(t)*, the total *X(T)* harmonic content is almost null, as a consequence the expected Adaptive Filter quick self-calibration is not achieved.

A possible solution could be represented by a pre-initialization of the filters coefficients, at pre-calculated optimized values, adapted to an initial compromise situation available to the widest range cases. Then, during the sliding phenomenon, the variations of the error *E(T)* at the correction input of the adaptive filter will be sufficient to perform the optimal correction of the coefficients in real time.

Nevertheless, the aim of the development is to achieve a total optimal self-tuning of the Adaptive Filter without any preliminary activity.

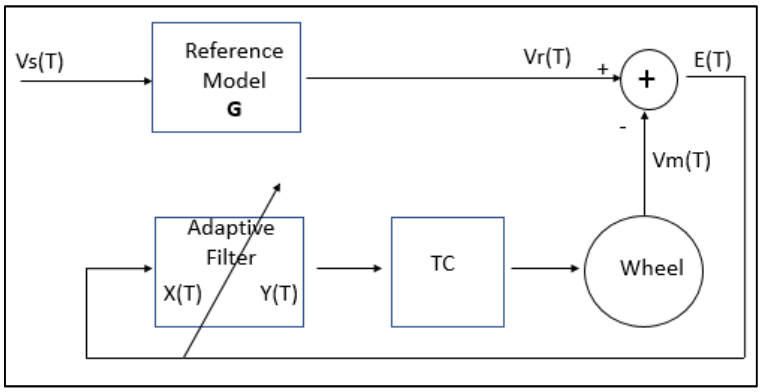

Figure 6: Least Mean Square adaptive filter applied on a slide control (modified architecture).

The solution to the problem is shown in Figure 6. The error *E(T)* itself contains the information of the target and of the fluctuation of the instantaneous speed *Vm(T)*. In the shown description, the error *E(T)* is not only used as a correction factor of the Adaptive Algorithm, but as input *X(T)* to the Adaptive Filter itself. The error *E(T)* has the harmonic content necessary for the expected fast auto-calibration, and at the same time contains the information necessary for the generation of the braking force corrections. The described solution allows a continuous fast dynamic calibration of the coefficients of the Adaptive Filter always starting from completely zeroed Adaptive Filters coefficients.

As previously reported, LMS Adaptive Filters are implemented using both Finite Impulse Response FIR and Infinite Impulse Response IIR structures. Both solutions have pro's and con's.

IIR advantage in this specific case is that it can assume a second order filter form. Therefore, few calculations are needed at every sampling period. In addition, in the second order implementation the IIR form contains the factor *1/s* representing the integrative component. The integrative factor helps in keeping memory of the needed torque when the error *E(T)* has reached the null value. On the opposite, IIR filter may be unstable under certain coefficients combination, which may cause unwanted instabilities in the overall system.

Despite FIR filters need higher calculation amount per sampling time, they are known to be intrinsically more stable, suitable for the proposed application. As a con's, FIR miss memory characteristic, needed to implement the integrative function. In case of a purely pneumatic torque control (pneumatic WSP) the integrative component can be provided by the brake cylinder functionality: the Adaptive Filter output *Y(T)* becomes an "air flow" demand, and the brake cylinder performs the integration transformation, from air flow to pressure.

In case of a more complex torque control, mixing pneumatic brake and electrodynamic brake, *Y(T)* must keep the torque demand form. A solution to the lack of an integrative component is shown in Figure 7 where a supplementary integrator, possibly equipped with a self-calibration method using a dedicated LMS cell, is placed in parallel to the FIR structure.

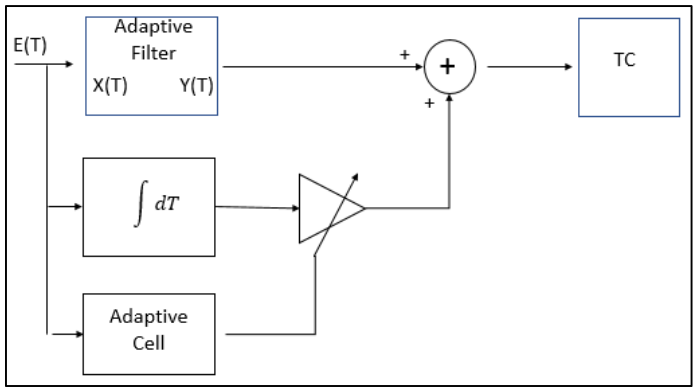

Figure 7: Adaptive filter applied on a torque control system (architecture including integral).

In order to keep the control always reactive to new variations of the external parameters of the system, the leakage function of the Adaptive Filters is used to perform a continuous de-tuning of the filter coefficients in error situations and *E(t)* close to zero, within, however, limits of variation of the coefficients such as to allow the self-calibration process to recover a correct calibration of said coefficients upon the reappearance of significant values of *E(t)*.

TESTING

The above described algorithm has been firstly implemented in a model-based environment, where a purely software mathematical model is in charge to simulate the train longitudinal dynamic, the brake torque actuators (valves, cylinders, calipers, friction pairs), the axle rotational dynamic and the wheel-rail contact. The model-based tests allow a sort of preliminary debug of the algorithm considering that the implementation of such algorithm in an embedded electronic system needs to overcome a series of problematics related to the limitation of resources (digital resolution) and the discrete time-period of tasks' execution.

In any case, this article will not focus on the preliminary virtual test of the adaptive algorithm, but a step forward wants to be done. The test environment consists not only of a classical test rig, implementing a virtual vehicle model, but also of a multi-axle roller rig reproducing the physical wheel-rail contact for four consecutive wheelsets.

The "Faiveley multi-axle roller rig" has been fully detailed in a previous work [7]. However, to maintain the consistency of this article a brief description of the machine will be reported.

MULTI-AXLE ROLLER RIG

The innovative patented design conceived by Faiveley Transport [7] is focalised on the capability to reproduce low adhesion conditions for a multiple wheels-rail contact (Figure 8). For this reason, the rail profile is fixed on the inner surface of the hollow cylinder, limiting the impact of centrifugal force on the contaminant layer. The four train wheels rotate on the rail surface, one after the other, offering the possibility to evaluate the rail's cleaning along the train's wheelsets. The geometrical scaling factor used for this machine is 1:5, both for the wheels' and rail's profile. The inner diameter of the rail is 2 meters, ten times the wheels' diameter: this ratio ensures a good approximation of the wheel-rail contact's geometry. The materials used for the wheels and the rail are identical to those used in Europe. Each wheel is equipped with its own:

- electrical motor, controllable using a speed or a torque reference, allowing the user to:

    - apply the desired braking or traction torque to the wheel
    - control the wheel at the desired rotational speed
- torque sensor, able to measure the torsional force exchanged between the motor and the wheel
- hydraulic load actuator, able to dynamically control the normal load that the wheel exerts on the rail surface
- load cell sensor, for the real-time measurement of the wheel's load on the rail

The roller's wheel (Figure 8) is driven by an electrical motor, controllable using a speed or a torque reference, allowing the user to:

- apply the desired braking or traction torque to the rotating rail (reproducing the desired train inertia/mass)
- control the roller at the desired rotational speed

The machine is capable to control the contamination of the rail, through the use of two devices:

1. Dispenser: in charge of injecting, in front of the first wheel, the contaminant/s on the rail (water, water and soap, oil, various friction modifiers, etc.)
2. Cleaner, in charge of cleaning the rail after the 4th wheel

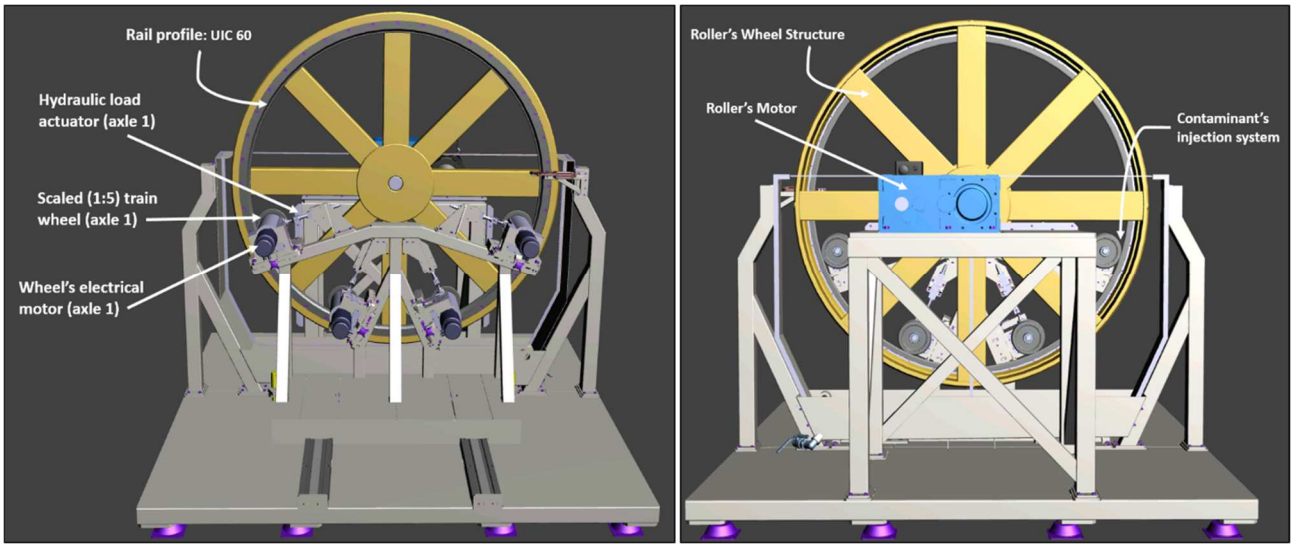

Figure 8: Faiveley Transport Roller Rig innovative design – 3D project – front side view (left) and back side view(right). The same configuration (wheel, motor, hydraulic actuator) is repeated for the four axles.

The experimental validation performed on the roller [7] confirmed the goodness of the structural approach used to design the machine. On one side, we ensured to have on board all the degrees of freedom (actuators, motors, control strategies, etc.) allowing to reproduce a generic train's mission profile in all its phases (traction, coasting, braking) and to replicate the train's braking distances. On the other side, we ensured that the choice of materials, scaling factors for geometries, forces and masses doesn't alter the friction coefficient on the contact area, for dry rail and water contamination.

RESULTS

The testing of the adaptive wheel slide protection algorithm on the multi-axle roller rig is the object of this section. The work flow aims to replicate the process usually adopted for train filed test (commissioning on train in commercial or testing track) and fully defined by the UIC 541-05 regulation. Once defined the tests' initial speed, usually close to the maximum vehicle speed, the nominal braking distance in dry condition is identified as the average distance resulting from a series of repeated braking test on track (this braking distance must be in line with the brake calculation

estimation). Once identified the *braking distance in dry condition*, the low adhesion test can start by recreating the low adhesion condition using a mixture of water and soap directly injected on the rail in front of the first axle of the train. The braking distance obtained with low adhesion are then compared with the *braking distance in dry condition*, on this comparison is based the evaluation of the WSP system performances. The UIC 541-05 regulation [8] provides all the details related to the test procedure giving an idea about the complexity of such test campaign. On the Faiveley multi-axle roller rig, the above described test procedure can be executed in few minutes with great advantages in terms of repeatability and time/cost effort. The following results represent an application's example of such test procedure for the adaptive wheel slide protection algorithm acting on the multi-axle roller rig. The roller rig has been configured (axles load, roller's motor inertia, initial speed) to reproduce a typical trailer coach, with a nominal deceleration in dry condition around *-1 m/s*^{2}.

The following figures (Figure 9, Figure 10, Figure 11) report the dynamic behaviour obtained on the roller, in dry condition.

Figure 9: Roller test - speeds profile in dry condition. The available adhesion is enough to guarantee the full rotation of the axles (the roller/train speed is equal to the axles speeds). Average deceleration is around -1 m/s2.

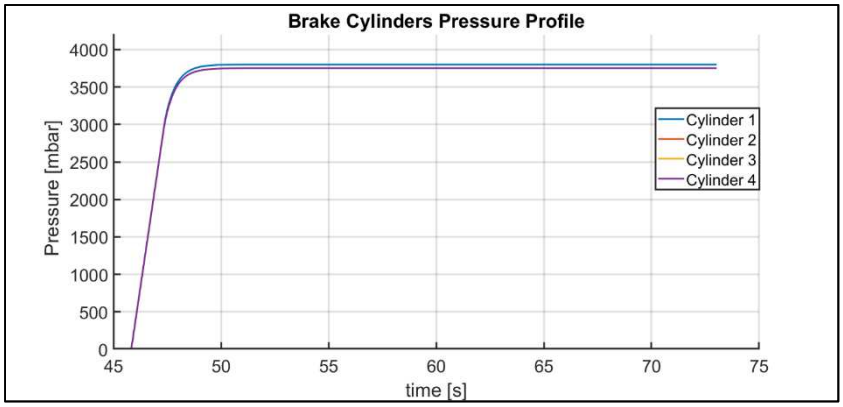

Figure 10: Roller test - cylinder pressure profile in dry condition. In this phase, the braking system is simulated (dump valves, cylinders, calipers, friction pairs) giving the conversion form cylinder pressure to motors' braking torque. Because the adhesion is high, no axles are sliding, no pressure reduction is requested by WSP.

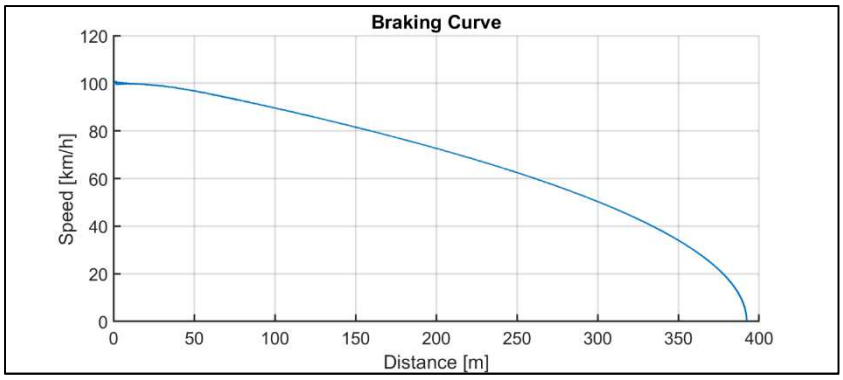

Figure 11: Roller test - braking curve for dry. The braking distance obtained in dry condition is 393 meters.

In order to complete the test procedure, the low adhesion condition is recreated on the roller by injecting water and soap contamination in front of the first wheel, using the dispenser set on a defined flow (*10 l/h*). The test described above for the dry condition has been repeated with the same dynamic parameters except the rail contamination. No tuning activity has been performed on WSP system.

The following figures (Figure 12, Figure 13, Figure 14) report the dynamic behaviour obtained on the roller, in wet condition.

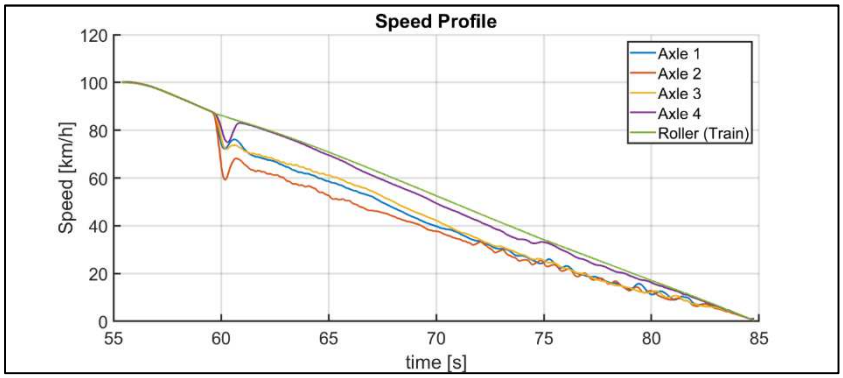

Figure 12: Roller test - speeds profile in wet condition. The available adhesion is not enough to allow the application of the nominal braking effort. ***The adaptive wheel slide protection modulates the braking effort and maintains the axle speeds at a controlled sliding.***

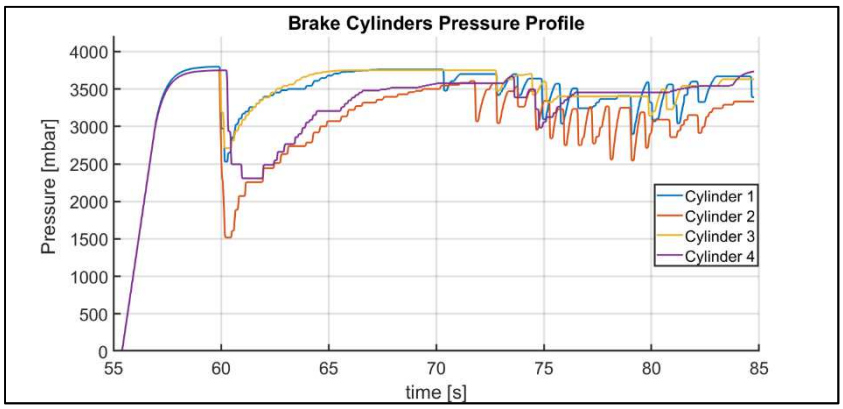

Figure 13: Roller test - cylinder pressure profile in wet condition. In this phase, the braking system is simulated (dump valves, cylinders, calipers, friction pairs) giving the conversion form cylinder pressure to motors' braking torque. ***The adaptive wheel slide protection modulates the cylinders pressure by controlling a couple of dump valves for each axle.***

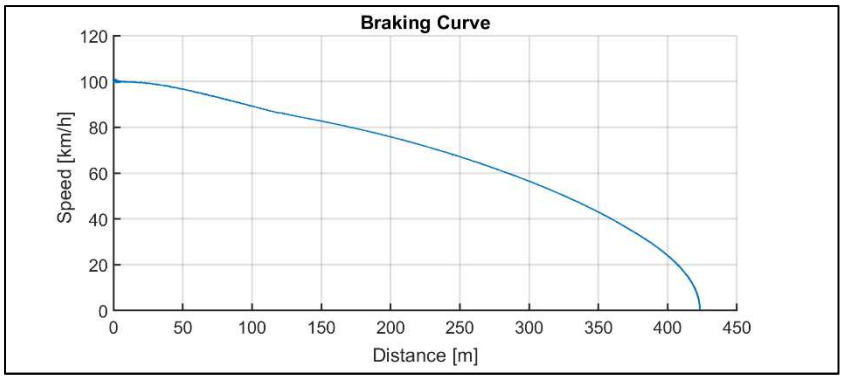

Figure 14: Roller test - braking curve for wet. The braking distance obtained in wet condition is 423 meters (+8% with respect to the dry braking distance).

The proposed test represents only an example of application of a certain methodology, testing the adaptive WSP algorithm acting on the multi-axle roller rig guarantying a high level of integration between simulated and physical functions.

This test, and all the test campaign performed with the proposed methodology, proves the capability of the adaptive algorithm to autonomously find its tuning and stably maintain the axles speed to a controlled sliding. Furthermore, the equivalent air consumption and the braking distances are widely within the limits of UIC 541-05 regulation.

CONCLUSION

In the first half of the article the objectives and the architecture of a self-adaptive wheel slide protection algorithm have been defined. The challenge to reduce and/or eliminate the tuning phase has been addressed using a mathematical approach based on LMS filter.

The performances of such self-adaptive WSP algorithm have been proven using the same approach proposed by UIC 541-05 regulation applied on the Faiveley multi-axle roller rig. After a brief description of the test environment (the multi-axle roller rig), the test methodology has been detailed and executed on an application case.

The achieved results are highly satisfactory and in-line with the UIC 541-05 rules in terms of braking distances and air consumption, proving the capability of the adaptive algorithm to autonomously find its tuning and stably maintain the axles speed to a controlled sliding.

Next step of this research is to compare the performances of a traditional wheel slide protection algorithm with the adaptive one in the same environmental conditions, giving a statistic coverage to this comparison on a wide range of adhesion levels.

BIBLIOGRAFIA

[1] Automatic Slip Control for Railway Vehicles, Daniel Frylmark and Stefan Johnsson, 6th February 2003

[2] Adaptive Fuzzy Sliding-Mode Control of Wheel Slide Protection Device for ER24PC Locomotive, Alireza Mousavi, Amir H. D. Markazi, Saleh Masoudi

[3] Application of Fuzzy Control Algorithms for Electric Vehicle Antilock Braking/Traction Control Systems, P. Khatun, C. M. Bingham, N. Schofield, and P. H. Mellor 2003

[4] Study on anti-slip regulation of quarter automobile based on PID control Qiang Fu, Lijie Zhao, Mingxiu Cai

[5] Adaptive Signal Processing, B.Widrow

[6] Method for controlling and recovering the adhesion of the wheels of a controlled axle of a railway vehicle, Roberto Tione, 2015

[7] M. Frea, S. Perna, "FIRST EXPERIMENTAL RESULTS FROM THE MULTI-AXLE ROLLER RIG IN DEGRADED RAIL ADHESION CONDITIONS", EuroBrake 2018 article n° EB2018-BSY-016, 14 pages, 2018

[8] UIC 541-05, 3rd edition March 2016